SCIENTIFIC REPORTS

OPEN

ADAP1 limits neonatal cardiomyocyte hypertrophy by reducing integrin cell surface expression

Hugo Giguère [1], Audrey-Ann Dumont[2], Jonathan Berthiaume[1], Vanessa Oliveira[3], Gino Laberge[3] & Mannix Auger-Messier [1,2,3]

The ArfGAP with dual PH domains 1 (ADAP) regulates the activation of the hypertrophic mitogen-activated protein kinase ERK1/2 pathway in non-cardiomyocytes. However, its role in cardiomyocytes is unknown. Our aim was to characterize the role of ADAP1 in the hypertrophic process of cardiomyocytes. We assessed the expression of ADAP1 in the hearts of adult and neonatal rats by RT-qPCR and Western blotting and showed that it is preferentially expressed in cardiomyocytes. Adenoviral-mediated ADAP1 overexpression in cultured rat neonatal ventricular cardiomyocytes limited their serum-induced hypertrophic response as measured by immunofluorescence microscopy. Furthermore, ADAP1 overexpression completely blocked phenylephrine- and Mek1 constitutively active (Mek1ca) mutant-induced hypertrophy in these cells. The anti-hypertrophic effect of ADAP1 was not caused by a reduction in protein synthesis, interference with the Erk1/2 pathway, or disruption of the fetal gene program activation, as assessed by nascent protein labeling, Western blotting, and RT-qPCR, respectively. An analysis of cultured cardiomyocytes by confocal microscopy revealed that ADAP1 partially re-organizes α-actinin into dense puncta, a phenomenon that is synergized by Mek1ca overexpression. Biotin labeling of cell surface proteins from cardiomyocytes overexpressing ADAP1 revealed that it reduces the surface expression of β1-integrin, an effect that is strongly potentiated by Mek1ca overexpression. Our findings provide insights into the anti-hypertrophic function of ADAP1 in cardiomyocytes.

ArfGAP with dual PH domains 1 (ADAP1), also known as centaurin-α1, is a GTPase-activating protein (GAP) that regulates the activity of small GTPases from the ADP-ribosylation factor (ARF) family[1]. ADAP1 was first identified in the brain and the heart, but its role in cardiac function was not investigated at the time[2]. ADAP1 interacts with nucleolin, Kif13b, and protein kinase C[3–5], and is also functionally linked with the activation of the mitogen-activated protein kinases (MAPKs) ERK1/2[6,7], which is of particular interest in a cardiac context, especially since the MEK1-ERK1/2 pathway supports and potentiates cardiac hypertrophy[8–10]. This signaling pathway is activated in response to several stresses in the heart, including hypertrophic agonist stimulation and mechanical stretching via integrins[11,12]. On the other hand, inhibiting ERK1/2 blocks the onset of hypertrophy in many cases[13,14]. ADAP1 also regulates small G protein ARF6 activity through its GAP domain, catalyzing the conversion of active ARF6-GTP to inactive ARF6-GDP[1,15,16]. In turn, ARF6 regulates different processes that occur in cell membranes, such as vesicular trafficking (endocytosis), membrane fusion/budding, and cytoskeletal reorganization[17–19].

Interestingly, ARF6 also regulates the surface expression and recycling of integrins in HeLa and endothelial cells[20,21]. Notably, Hongu *et al.* showed that ARF6 is required for hepatocyte growth factor-induced endothelial cell spreading and β1-integrin recycling[21]. Integrins do not simply act as inert anchors of cells to the extracellular

[1]Département de Pharmacologie et Physiologie, Faculté de Médecine et des Sciences de la Santé, Université de Sherbrooke, Sherbrooke, QC, Canada. [2]Département de Biochimie, Faculté de Médecine et des Sciences de la Santé, Université de Sherbrooke, Sherbrooke, QC, Canada. [3]Département de Médecine – Service de Cardiologie, Centre de Recherche du CHUS, Faculté de Médecine et des Sciences de la Santé, Université de Sherbrooke, Sherbrooke, QC, Canada. Correspondence and requests for materials should be addressed to M.A.-M. (email: Mannix.Auger-Messier@USherbrooke.ca)
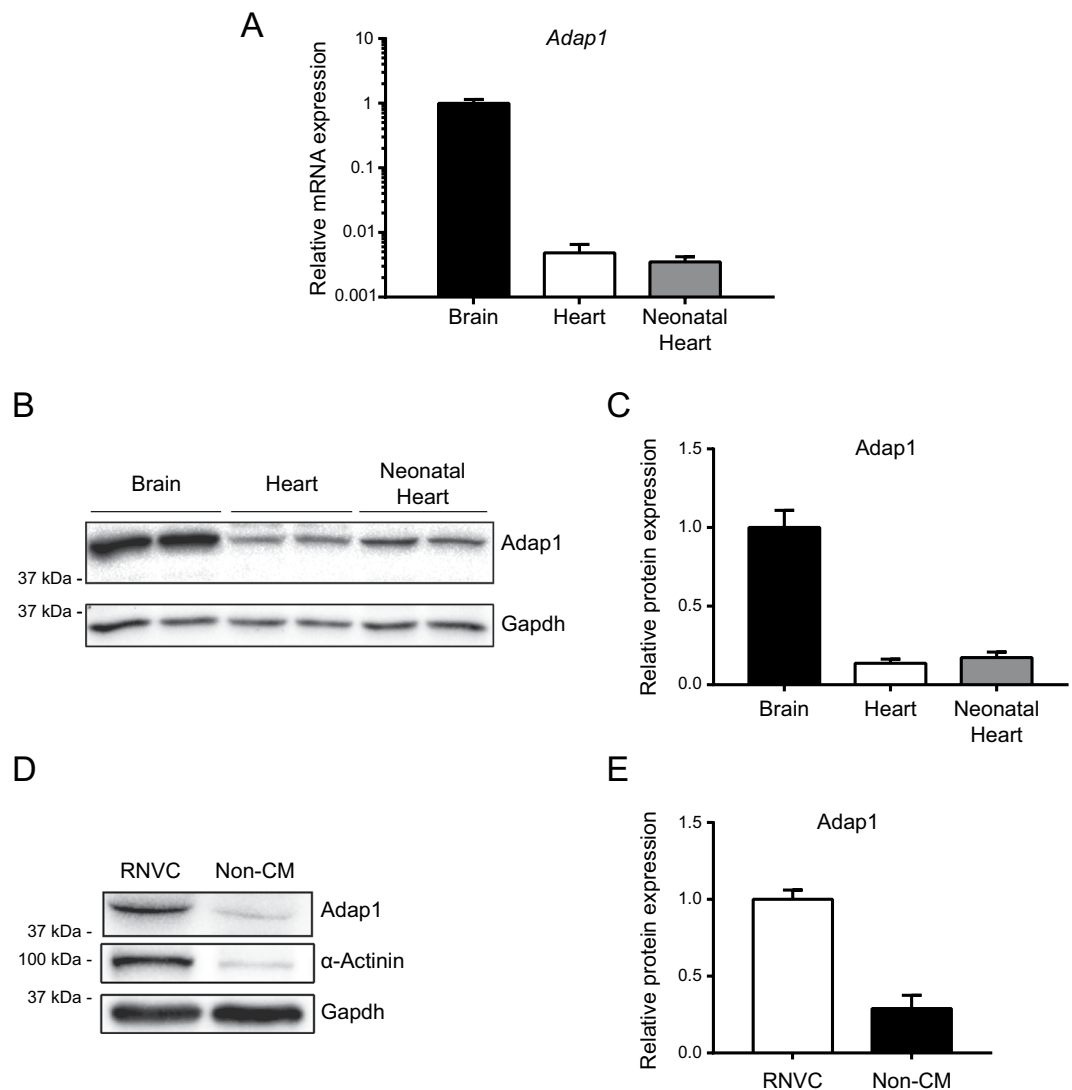
1

Figure 1. Adap1 expression in cardiac cells. (**A**) Relative levels of *Adap1* mRNA expression in the rat brain (adult) and heart (adult and 2-day-old neonate) were measured by RT-qPCR and were normalized to the *Rpl30* reporter gene (*n* = 4 independent tissues). (**B**) Representative Western blots of Adap1 and Gapdh (loading control) detected from whole brain and heart extracts. (**C**) The histogram represents the relative expression level of Adap1 normalized to Gapdh in the respective tissues (*n* = 4 independent tissues). (**D**) Representative Western blot of Adap1, α-Actinin (cardiomyocyte specific marker), and Gapdh (loading control) detected in the protein lysates of enriched rat neonatal ventricular cardiomyocytes (RNVC) and non-cardiomyocytes (Non-CM). (**E**) The histogram represents the relative expression level of Adap1 normalized to Gapdh in the respective cell lysates (*n* = 4 independent cell isolations). Full-length blots are presented in Supplementary Fig. 1.

matrix, they also play an active role in the hypertrophic process of cardiomyocytes[22,23]. Indeed, β1-integrin over-expression in cultured cardiomyocytes promotes cell hypertrophy[24], while down-regulation of β1-integrin at the surface of cardiomyocytes impedes such hypertrophy[25].

Based on these potential signaling mechanisms, we hypothesized that ADAP1 may regulate cardiomyocyte hypertrophy by interfering with integrin-dependent processes. We show for the first time that ADAP1 can block cardiomyocyte hypertrophy *in vitro* by reducing the expression of β1-integrin at the cell surface.

Results

Adap1 is expressed in cardiomyocytes.

When ADAP1 was first cloned, one clue suggested that it is expressed to some extent in the hearts of adult rats[2]. In order to validate this observation, we analyzed the cardiac expression of Adap1 in Sprague Dawley rats. Compared to the level of *Adap1* mRNA expression observed in the brain, *Adap1* mRNA transcripts were expressed at the relative levels of 0.5% and 0.35% in the hearts of adult and neonatal rats, respectively (Fig. 1A). The presence of an *Adap1* transcript in whole heart extracts was also confirmed by end-point PCR detection of putative splice variants that display the same unique transcript detected in whole brain extracts (data not shown). As expected, Western blotting analyses confirmed that whole
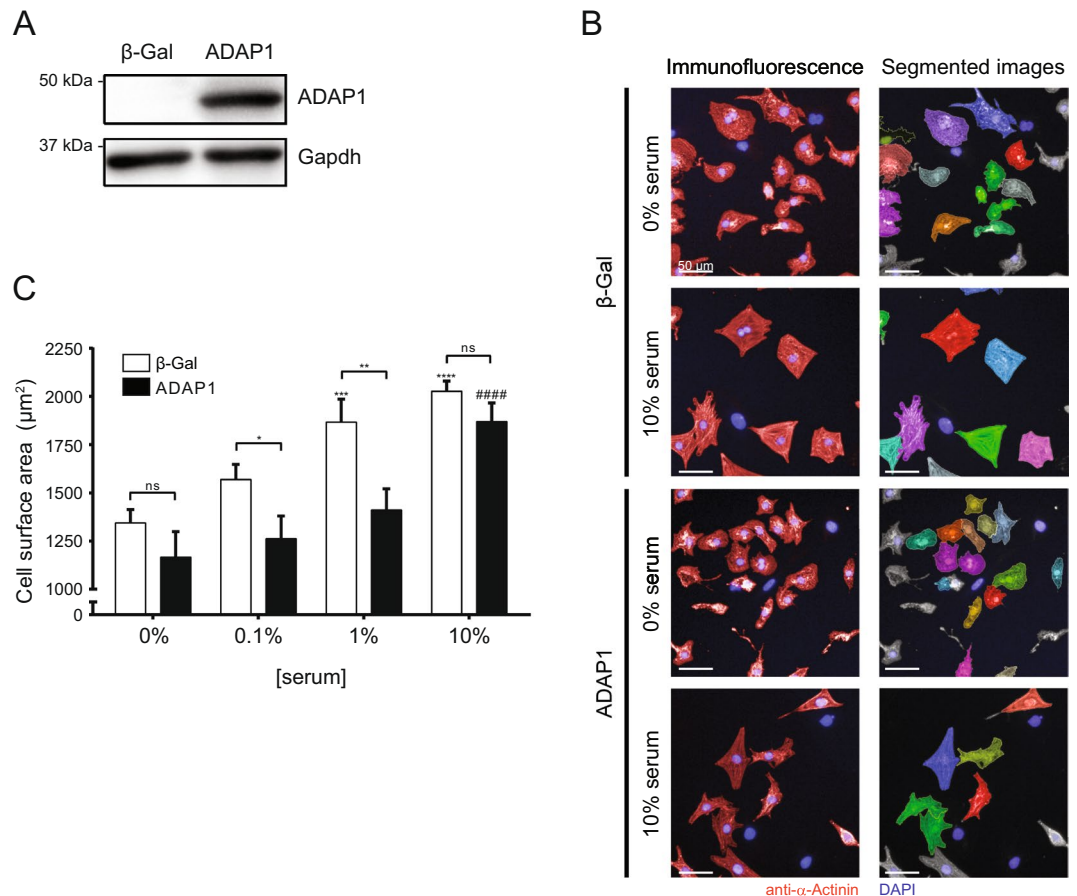
Figure 2. ADAP1 restrains the serum-induced increase in cell size of cultured cardiomyocytes. (**A**) Western blot detection of adenovirus-mediated 3xFLAG-hADAP1 overexpression (MOI of 50) in rat neonatal ventricular cardiomyocytes (RNVC) cultured for 72 h post-infection. (**B**) RNVC were infected with either β-Gal- (negative control) or ADAP1-overexpressing adenovirus and were cultured for 72 h in the absence (0%) or presence (10%) of serum. Representative images of α-Actinin-immunostained RNVC (left) and corresponding segmented images were acquired using the Operetta High-Content Imaging System (Perkin Elmer). The scale bar represents 50 μm. (**C**) The histogram represents the cell surface areas of RNVC overexpressing either β-Gal or ADAP1 and cultured for 72 h with increasing concentrations of serum ($n = 3$ independent experiments). *$P < 0.05$ and **$P < 0.005$ vs. β-Gal; ***$P < 0.0005$ and ****$P < 0.0001$ vs. β-Gal at 0% [serum]. ####$P < 0.0001$ vs. ADAP1 at 0% [serum]; ns, not significant; Two-way ANOVA with Sidak's multiple comparison test. Full-length blots are presented in Supplementary Fig. 2.

brain lysates contained high levels of Adap1 (Fig. 1B). Interestingly, Adap1 was also detected in whole heart extracts of adult and neonatal rats at levels relative to the brain of 13% and 17%, respectively (Fig. 1B,C). A similar expression profile was also obtained using another antibody targeting a different immunogen sequence of Adap1 (data not shown). Since the heart is composed of different cells, including cardiomyocytes, endothelial cells, and fibroblasts[26], we determined which of these cell types preferentially expressed Adap1. As measured by Western blotting, Adap1 was 3-fold more abundant in isolated rat neonatal ventricular cardiomyocytes (RNVC) than in partially enriched non-cardiomyocyte (non-CM) cells (Fig. 1D,E), suggesting that it likely plays a role in cardiomyocytes.

ADAP1 hinders the hypertrophy of cardiomyocytes. The overexpression of ADAP1 affects the cytoskeletal organization of epithelial HeLa cells and increases dendritic filopodia formation by primary cultured hippocampal neurons[1,16]. Since the reorganization of the cytoskeleton of cultured cardiomyocytes mediates their hypertrophic response to external stimuli[27], we hypothesized that ADAP1 overexpression might affect the serum-induced increase in size of RNVC. Western blotting analyses confirmed that efficient adenoviral-mediated overexpression of ADAP1 occurs in cultured RNVC (Fig. 2A). We imaged α-actinin-immunostained RNVC and measured their cell surface area (highlighted as segmented images in Fig. 2B) following a 72-h incubation with increasing serum concentrations. In the absence of serum, RNVC overexpressing ADAP1 tended to be smaller than control cells infected with adβ-Gal, although the difference was not significant (Fig. 2B,C). While the size of adβ-Gal-infected RNVC increased significantly and dose-dependently in response to serum, ADAP1 limited the hypertrophic response of RNVC to this external stimulus. In fact, ADAP1 prevented any significant increase in

the cell surface area of RNVC cultured with 0.1% and 1% serum. However, 10% serum was sufficient to increase the cell size of ADAP1-overexpressing RNVC to approximately the same extent as control cells (Fig. 2B,C). Although the overexpression of ADAP1 did not significantly change the serum-induced regulation of *Myh6* and *Myh7* mRNA expression, it delayed the upregulation of *Nppa* transcript level in response to increasing serum concentration (data not shown) and corroborated with the corresponding cell size.

The serum and phenylephrine pro-hypertrophic stimulus do not regulate the expression of endogenous *Adap1* at the transcriptional and translational levels in RNVC (data not shown). Interestingly, the overexpression of ADAP1 completely blocked the phenylephrine-induced hypertrophy of RNVC (Fig. 3A). Since both serum- and phenylephrine-dependent responses in cardiomyocytes commonly converge toward the hypertrophic MEK1-ERK1/2 signaling pathway[10], we investigated how ADAP1 would impact the effect on RNVC cell size of overexpressing a Mek1 constitutively active mutant (Mek1ca). ADAP1 not only completely blocked the Mek1ca-induced hypertrophy of RNVC, it significantly reduced their size even further compared to adβ-Gal-infected control cells (Fig. 3B). However, the 2-fold acceleration in the rate of Mek1ca-induced protein synthesis (Fig. 3C,D) and the increase in Erk1/2 phosphorylation (Fig. 3E,F) were not inhibited nor altered by the overexpression of ADAP1, suggesting that ADAP1 potently impedes other components of the hypertrophic process in cardiomyocytes.

ADAP1 does not interfere with the fetal gene program.

The hypertrophic response of cardiomyocytes is often associated with the re-expression or repression of genes corresponding to the fetal stage of cardiac development[28,29]. While Mek1ca overexpression in RNVC triggers the fetal gene program, the activation of the program, as well as cardiomyocyte hypertrophy, are abrogated by the genetic or pharmacological inhibition of the MEK1-ERK1/2 pathway[30–33]. In our experimental conditions, the infection of RNVC with adMek1ca provokes a 60% decrease in *Myh6*, *Mef2c*, and *Gata4* mRNA expression (Fig. 4A,D,E) and a 40% decrease in *Srf* (Fig. 4F) mRNA expression. The *Myh7* gene was not significantly affected by Mek1ca overexpression (Fig. 4B) while the expression of the *Nppa* gene was increased over 10-fold (Fig. 4C). In addition, the expression of the calcium signaling-related genes *Cacna1c*, *Atp2a2*, and *Pln* was reduced by more than 75% in the presence of Mek1ca (Fig. 4G–I). More importantly, the co-expression of ADAP1 and Mek1ca did not significantly affect any of these changes in gene expression compared to the overexpression of Mek1ca alone. These results suggest that the anti-hypertrophic effect of ADAP1 is dominant over Mek1ca-mediated transcriptional regulation.

ADAP1 regulates α-actinin organization and β1-integrin cell surface expression.

A careful examination of immunostained RNVC revealed that the overexpression of both ADAP1 and Mek1ca have a significantly greater impact on α-actinin organization than in control adβ-Gal-infected RNVC. Indeed, higher definition imaging by confocal microscopy revealed that the combined overexpression of ADAP1 and Mek1ca in RNVC induces the formation of multiple α-actinin dense puncta (Fig. 5A). Interestingly, ADAP1 or Mek1ca alone also induced, to some extent, the formation of such large, distinct cytoskeletal structures while control adβ-Gal-infected RNVC did not (Fig. 5A). Increasing the overexpression of ADAP1 up to a multiplicity of infection (MOI) of 100 did not further increase the number of α-actinin puncta (data not shown). More importantly, quantifying the number of these α-actinin puncta per cell using the Operetta High-Content Imaging System revealed that the combined overexpression of ADAP1 and Mek1ca has a synergistic effect in RNVC (Fig. 5B).

Given that the activation of the Mek1-Erk1/2 signaling pathway in RNVC increases the expression of integrins and modulates their localization at the cell surface, promoting hypertrophy[34], we hypothesized that ADAP1 may interfere with these processes. Indeed, cell surface biotin labeling indicated that ADAP1 by itself significantly reduces the localization of β1-integrin at the surface of RNVC without changing the total expression of β1-integrin (Fig. 6A,B). Strikingly, β1-integrin was almost completely absent from the surface of RNVC overexpressing both ADAP1 and Mek1ca (Fig. 6A,B), indicating that ADAP1 impairs the processes required for the normal expression of β1-integrin at the surface of RNVC.

Among the β1-integrin-associated proteins forming the cardiac costameres, it is interesting to note that the adaptor protein Hic-5, a paxillin family member, is essential for the hypertrophic process of cultured RNVC[35]. To gain a mechanistic insight into the ADAP1 anti-hypertrophic effect, we verified how ADAP1 impacts Hic-5 expression in RNVC. The overexpression of ADAP1, alone or combined with Mek1ca, reduced Hic-5 expression levels to approximately 65% and 50%, respectively, compared to control adβ-Gal-infected RNVC (Fig. 6C,D). Altogether, these results suggest that ADAP1 interferes with the formation of these signaling hubs, which are required for cardiomyocyte hypertrophy.

Discussion

In the present study, we identified and characterized, for the first time, the role of Adap1 in cardiomyocytes. We showed that (i) Adap1 is present in both neonatal and adult rat hearts and that it is predominantly expressed in cardiomyocytes, (ii) the overexpression of ADAP1 restrains the development of serum-induced hypertrophy and completely blocks Mek1ca-induced hypertrophy in cultured RNVC, and (iii) ADAP1 reduces the localization of β1-integrin at the cardiomyocyte surface and, as such, the hypertrophic process of cardiomyocytes.

Adap1 mRNA and protein are expressed by a variety of neurons, including cortical, cerebellar, and hippocampal neurons, with peak mRNA expression reached between two and four weeks postnatally in rats[36]. While Adap1 is highly expressed in the whole brain, little is known about its expression in other tissues[2,36,37]. While a few indications suggest that Adap1 may be expressed in the heart, this possibility has not been verified or studied in detail. For instance, a protein expressed in both the brain and heart tissues of adult rats was detected by photoaffinity labeling with an inositol 4-phosphate analog, which led to the cloning of Adap1[2]. The Human Protein Atlas also indicates that ADAP1 has been detected by immunohistochemistry in the cardiomyocytes of adult heart specimens[38].
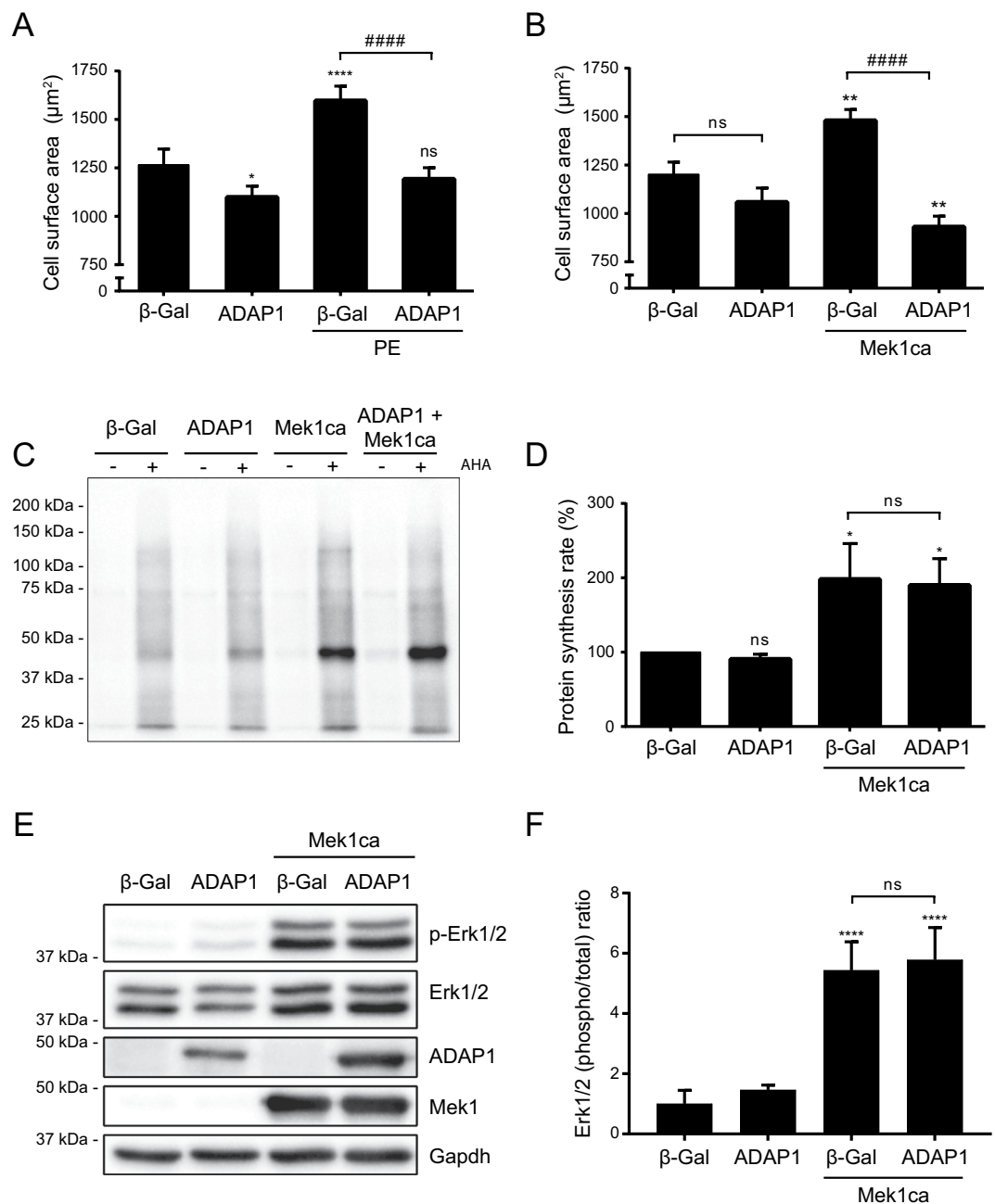
Figure 3. ADAP1 blocks phenylephrine- and Mek1ca-induced hypertrophy. Cell surface area measurements of rat neonatal ventricular cardiomyocytes (RNVC) overexpressing ADAP1 in the absence or presence of 50 μM phenylephrine (**A**) or Mek1ca-overexpressing adenovirus (**B**) compared with an adβ-Gal-infected control. Quantification of at least 3 independent experiments expressed as means ± SD. *$P < 0.05$; **$P < 0.005$; ****$P < 0.0001$ vs. unstimulated β-Gal. ####$P < 0,0001$ vs. stimulated β-Gal; ns, not significant; One-way ANOVA with Tukey's multiple comparison test. (**C**) Representative Western blots of protein lysates from adβ-Gal-, adADAP1-, or adMek1ca-infected RNVC metabolically labeled for 2 h with L-azidohomoalanine (AHA) and detected with biotin-alkyne and streptavidin-HRP. (**D**) The histogram represents the rates of nascent protein synthesis relative to the β-Gal control, which were measured using the same experimental conditions as in **C** ($n = 3$ independent experiments). *$P < 0.05$ vs. β-Gal; ns, not significant; One-way ANOVA with Tukey's multiple comparison test. (**E**) Representative Western blots of Erk1/2 phosphorylation status, ADAP1 and Mek1ca overexpression levels, and Gapdh (loading control) from protein lysates of RNVC cultured for 72 h following the indicated adenoviral infection. (**F**) The histogram represents the phospho/total Erk1/2 ratios relative to the β-Gal control and which were measured using the same experimental conditions as in **E** ($n = 4$ independent experiments). ****$P < 0.0001$ vs. β-Gal; ns, not significant; One-way ANOVA with Tukey's multiple comparison test. Full-length blots are presented in Supplementary Fig. 3.
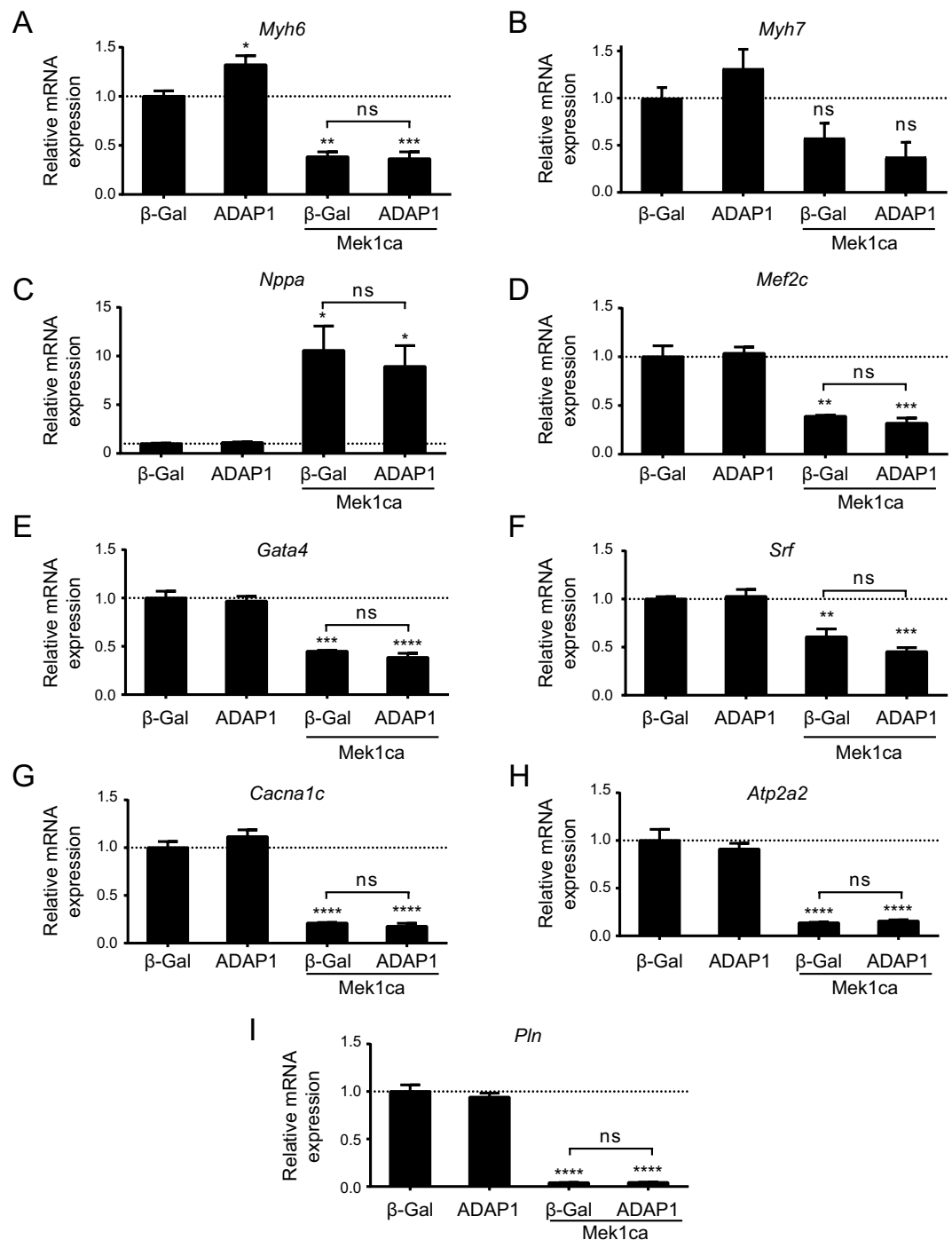
Figure 4. ADAP1 does not interfere with Mek1ca-induced fetal gene program activation. (**A**–**I**) Analysis by RT-qPCR of different mRNA expressed in rat neonatal ventricular cardiomyocytes (RNVC) that are representative of the fetal gene program. The RNVC were infected with an β-Gal- (negative control), ADAP1-, or Mek1ca-overexpressing adenovirus, individually or in combination as indicated, and were cultured for 72 h post-infection. The histograms represent mRNA expression levels relative to the β-Gal control and normalized to the *Rpl30* reporter gene (*n* = 3 independent experiments). *$P < 0.05$; **$P < 0.005$; ***$P < 0.0005$; ****$P < 0.0001$ vs. β-Gal; ns, not significant; One-way ANOVA with Tukey's multiple comparison test.

To further validate these observations, we showed that Adap1 is indeed expressed at similar levels in the hearts of neonatal and adult rats. As previously reported[2,36,37], we showed that the *Adap1* transcript is highly expressed in the brain of adult rats but is much less abundant in other tissues such as the heart. Nonetheless, we easily detected the Adap1 protein by Western blotting in whole heart extracts, suggesting that factors other than low transcript levels may mediate the high expression in cardiac tissue. This would be in agreement with the significantly slower turnover rate and longer metabolic half-life (t½ = 6.93 days) of Adap1 reported in primary
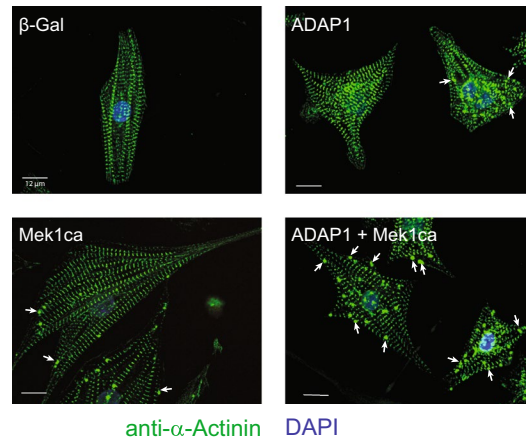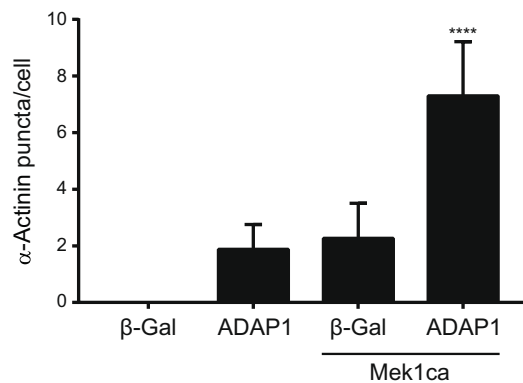
Figure 5. ADAP1 relocalizes cytoskeletal α-Actinin. (**A**) Representative confocal images (Olympus FluoView FV1000 microscope) of α-Actinin-immunostained rat neonatal ventricular cardiomyocytes (RNVC) infected with a β-Gal- (negative control), ADAP1-, or Mek1ca-overexpressing adenovirus, individually or in combination as indicated, and cultured for 72 h post-infection. Arrows point to α-Actinin dense puncta. The scale bar represents 12 μm. (**B**) Number of α-Actinin puncta per cell measured with the Operetta High-Content Imaging System (Perkin Elmer) using the same experimental conditions as in **A** ($n = 4$ independent experiments). ****$P < 0.0001$ vs. β-Gal; One-way ANOVA with Tukey's multiple comparison test.

cultures of cortical neurons[39]. Like the unique *Adap1* transcript variant detected in both brain and heart extracts by end-point PCR, the band of Adap1 protein expressed in these tissues migrated at the same molecular weight (43 kDa) previously reported for Adap1[2,40]. Since Adap1 was more abundantly expressed in isolated RNVC than in partially enriched non-cardiomyocytes cells, these findings suggest that it might contribute to cardiomyocyte development or function.

Adap1 functionally interacts with MAPKs Erk1/2 to activate this signaling pathway in COS-7 cells and hippocampal neurons through mechanisms that are not fully understood[6,7,41]. Since increased signaling of the Mek1-Erk1/2 axis induces cardiomyocyte hypertrophy[9,30,42], we hypothesized that ADAP1 might significantly promote the hypertrophic process in these cells. To verify this hypothesis, we overexpressed ADAP1 in RNVC but did not observe a significant increase in Erk1/2 phosphorylation under basal conditions. In addition, an acute stimulation with phenylephrine, a hypertrophic agonist, activated Erk1/2 more efficiently in RNVC over-expressing ADAP1 (data not shown). However, rather than increasing the size of cardiomyocytes in the absence of serum, ADAP1 caused a slight reduction in their cell surface area compared to adβ-Gal-infected control cells. Although an anti-hypertrophic effect was also observed at lower serum concentrations (0.1 and 1%), RNVC overexpressing ADAP1 were still able to hypertrophy in response to a higher concentration of serum (10%). This may be explained by the fact that serum contains several active factors able to induce cardiomyocyte hypertrophy through different Erk1/2-dependent and -independent signaling pathways[43–45].

We thus overexpressed the hypertrophic Mek1ca mutant in RNVC to determine whether sustained specific Erk1/2 activation could overcome the anti-hypertrophic effect of ADAP1. As expected, Mek1ca increased the cell size and protein synthesis rate of RNVC, which are hallmarks of cardiomyocyte hypertrophy, in our culture conditions. Interestingly, its co-expression with ADAP1 further reduced the cell surface area of RNVC to a significantly smaller size than that of adβ-Gal-infected control cells. The dominant effect of ADAP1 over
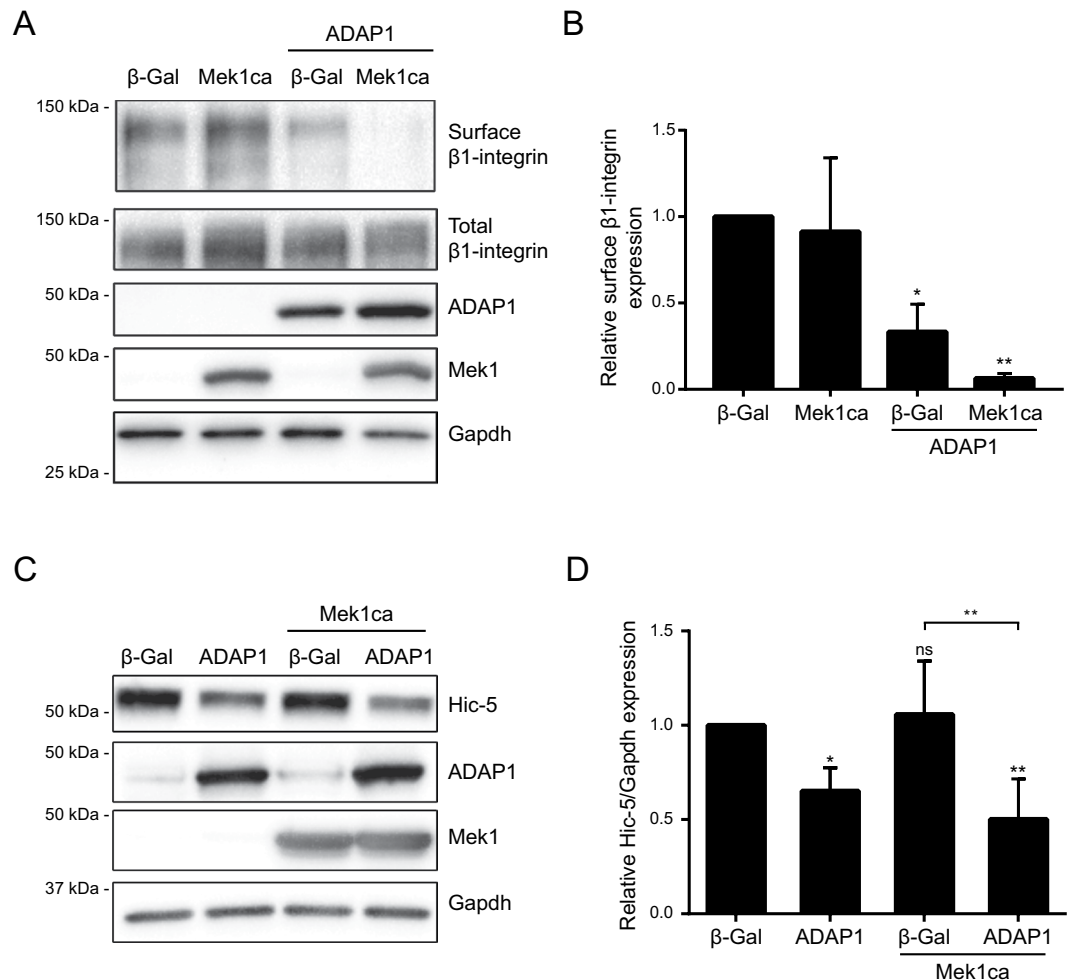
Figure 6. ADAP1 reduces cell surface β1-integrin expression in cardiomyocytes. (**A**) Representative Western blot of biotin-labeled cell surface β1-integrin expression compared to total β1-integrin expression in protein lysates of rat neonatal ventricular cardiomyocytes (RNVC) infected with a β-Gal- (negative control), ADAP1-, or Mek1ca-overexpressing adenovirus, individually or in combination as indicated, and cultured for 72 h post-infection. The expression levels of ADAP1, Mek1ca, and Gapdh (loading control) were also verified. (**B**) The histogram represents the level of cell surface β1-integrin expression normalized to total β1-integrin expression relative to the β-Gal control and measured using the same experimental conditions as in **A** ($n = 3$ independent experiments). *$P < 0.05$; **$P < 0.005$ vs. β-Gal; One-way ANOVA with Tukey's multiple comparison test. (**C**) Representative Western blot of Hic-5, ADAP1, Mek1ca, and Gapdh (loading control) in protein lysates obtained from RNVC cultured for 72 h following the indicated adenoviral infection. (**D**) The histogram represents the relative expression levels of Hic-5 normalized to Gapdh, relative to the β-Gal control, and measured under the same experimental conditions as in **C** ($n = 4$ independent experiments). *$P < 0.05$; **$P < 0.01$ vs. β-Gal; ns, not significant; One-way ANOVA with Fisher's LSD test. Full-length blots are presented in Supplementary Fig. 6.

Mek1ca-induced cardiomyocyte hypertrophy was not due to the normalization of the protein synthesis rate nor to Erk1/2 phosphorylation, which would have been surprising given the propensity of ADAP1 to favor Erk1/2 signaling. In addition, ADAP1 did not interfere with the Mek1ca-induced activation of the fetal gene program, another hallmark of *in vitro* and *in vivo* cardiomyocyte hypertrophy and which is regulated in part by Erk1/2 signaling[28,29,46,47]. Compared to previous reports[10,30,48], the broader transcriptional profile analysis performed in the current study is the first, to our knowledge, to examine more broadly the particular Mek1ca-induced fetal gene program in cultured rat neonatal ventricular cardiomyocytes. Taken together, these results suggest that ADAP1 interferes with an Erk1/2-independent mechanism to block Mek1ca-induced hypertrophy in RNVC.

Since ADAP1 overexpression modifies cytoskeleton organization in other cell types[1,49], we determined, by confocal microscopy, whether it has a similar effect in cardiomyocytes. The overexpression of ADAP1 significantly increased the formation of α-actinin dense puncta in RNVC. Strikingly, the co-expression of ADAP1 and Mek1ca synergistically increased the number of α-actinin puncta per cell, suggesting that both signaling molecules are involved in a common cytoskeletal reorganization mechanism. In addition to being a major cytoskeletal component of the sarcomeric Z-line, α-actinin also links the sarcomere with the extracellular matrix through integrins[50]. This prompted us to determine whether ADAP1 affects the expression of β1-integrin at the

cardiomyocyte surface since these integral membrane proteins regulate processes involved in cardiac hypertrophy[21–23]. Indeed, ADAP1 significantly decreased the expression of β1-integrin in the sarcoplasmic membrane while its co-expression with Mek1ca almost completely eliminated its expression at the surface of cardiomyocyte.

Cardiac costamer components such as paxillin also influence the internalization/recycling of integrin and the cardiomyocyte hypertrophic process[51]. For instance, the adaptor protein Hic-5, a paxillin family member, is essential for phenylephrine-induced hypertrophy of cultured RNVC[35]. We thus hypothesized that ADAP1 may interfere with Hic-5. We showed that the overexpression of ADAP1, alone or together with Mek1ca, significantly reduces Hic-5 protein expression in RNVC. Although Mek1ca-induced Erk1/2 phosphorylation seemed to be unaffected by the overexpression of ADAP1 in RNVC, we cannot exclude the possibility that the localization of activated Erk1/2 in specific subcellular compartments may have changed under these conditions, leading to an enhancement of α-actinin puncta formation and a reduction of Hic-5 expression and β1-integrin levels on the cell surface.

These results are in agreement with the opposing effects exerted by different Arf GAPs with regard to integrin signaling, internalization, and recycling[52]. For example, GIT1 and ACAP1 regulate the signaling of integrins in different cell types[53–55]. PAG3, another centaurin family member, interacts with paxillin and inhibits its recruitment at the integrin-rich focal adhesion complex[56]. Interestingly, after stimulating RNVC with the hypertrophic agonist endothelin-1, paxillin forms puncta structures that are similar to those observed in the present study[57]. The scaffold protein IQGAP1 also recruits melusin and focal adhesion kinase at a multiprotein complex required for Erk1/2-mediated cardiomyocyte hypertrophy[58]. Lastly, another interesting possibility arose from the demonstration that ADAP1 overexpression in HEK293 cells inhibits both basal and agonist-induced internalization of β2-adrenergic receptors[15]. While integrin internalization/recycling processes are different than G protein-coupled receptor trafficking, it would be interesting to determine whether Adap1 also regulates the expression of ion channels and proteins such as GPCRs at the surface of cardiomyocytes.

Collectively, these results provide new insights into the regulation of *in vitro* cardiomyocyte hypertrophy by Adap1 via the regulation of β1-integrin complexes. *In vivo* studies will be needed to further characterize the anti-hypertrophic function of Adap1 in cardiomyocytes exposed to physiological and pathological stresses.

Methods

Ethics. All animal procedures complied with NIH guidelines and were approved by the Université de Sherbrooke Institutional Committee for the Use and Care of Laboratory Animals.

Adenovirus generation.]The adenoviruses encoding the β-galactosidase (β-Gal) and Mek1 constitutively active mutant (Mek1ca) were generous gifts from Jeffery D. Molkentin (HHMI, Cincinnati, OH, USA). The seamless assembly and subcloning of 3xFLAG-tagged hADAP1 cDNA (Cat. #11033; DF/HCC DNA Resource Core) into the Gateway pENTR3C Dual Selection vector (Invitrogen) was performed with a NEBuilder HiFi DNA Assembly Cloning kit (New England Biolabs). The recombination with the Gateway pAd/CMV/V5-DEST adenovirus vector (Invitrogen) was performed using the Gateway LR Clonase II Enzyme Mix (Invitrogen). After linearizing the vector with PacI (New England Biolabs), 4 μg of digested product was transfected into 90–100% confluent HEK 293 A cells grown in 35-mm dishes using Lipofectamine 2000 transfection reagent (Invitrogen). After 6–8 days of culture, the adenovirus was collected from lysed cells and was amplified by transferring 100 μL of the primary stock to a 10-cm dish of 90–100% confluent HEK 293 A cells. The cells and supernatant were collected 48–72 h later, freeze-thawed three times, and centrifuged at 100 RCF for 5 min to remove cell debris. The supernatant was collected, aliquoted, and stored at –80 °C. Serial dilutions of each adenovirus were used to infect HEK 293 A cells and determine their respective titers. Hexon-expressing cells immunostained using anti-hexon antibody (ab8249; Abcam) were quantified 36 h post-infection.

Rat neonatal ventricular cardiomyocyte isolation and culture. RNVC were extracted from the hearts of Sprague Dawley rat pups (strain code 001; Charles River) 1–3 days after birth using the Neonatal Cardiomyocyte Isolation System (Worthington Biochemical Corporation). After decapitation, the hearts were removed, the atria were discarded, and the ventricles were cut in half. The isolated ventricles were incubated in calcium/magnesium-free Hank's Balanced Salt Solution containing trypsin (50 μg/mL) in vented-cap tubes with slow agitation at 4 °C for 18 h. The trypsin was then inhibited by adding Soybean Trypsin Inhibitor (200 μg/mL), and the ventricles were further digested with collagenase (100 units/mL) at 37 °C for 30 min. Following trituration and filtration through a 70-micron cell strainer, the cells were pre-plated on 10-cm dishes at 37 °C for 30 min to reduce non-cardiomyocyte contamination. Enriched RNVC were resuspended in M199 medium containing 10% fetal bovine serum (FBS), 2 mM glutamine, 100 U/mL of penicillin, and 100 μg/mL of streptomycin. They were then plated at a density of 43,000 cells/cm² on fibronectin-coated microplates for immunofluorescence or on gelatin-coated cell-culture dishes for other experiments. Five hours after plating, the RNVC were infected with the appropriate adenoviruses at an MOI of 50 and were cultured in a humidified incubator with 5% CO_2 at 37 °C for 72 h before analysis.

Real-time PCR. Total RNA was extracted from RNVC using RNeasy Mini kits (Qiagen) according to the manufacturer's protocol. ProtoScript II Reverse Transcriptase (New England Biolabs) was used to prepare cDNA from 1000 ng of total RNA in 20 μL. Real-time PCR was performed on technical duplicates with cDNA diluted 30x in nuclease-free water supplemented with SsoAdvanced Universal SYBR Green Supermix (Bio-Rad) using a Mastercycler ep RealPlex (Eppendorf). Data were normalized to *Rpl30* and fold changes were obtained using the $2^{(-\Delta\Delta Ct)}$ method[59]. Primer sequences are given in Table 1.

Western blotting analysis. Proteins were extracted from cultured RNVC using RIPA lysis buffer containing 50 mM Tris-HCl (pH 7.4), 150 mM NaCl, 1% Triton X-100, 1% sodium deoxycholate, 0.1% SDS, 1 mM

Gene name	Gene description	Sequences (5′->3′)
Rpl30	Ribosomal protein L30	Fwd: TCTTGGCGTCTGATCTTGGT
		Rev: AAGTTGGAGCCGAGAGTTGA
Adap1	ArfGAP with dual PH domains 1	Fwd: CAAAGACCCTCTGGATGCCTT
		Rev: GGTGACTCTGGGTTGACGG
Myh6	Myosin heavy chain 6	Fwd: GGCCAAGAGCCGTGACATT
		Rev: TTGTGGGATAGCAACAGCGAG
Myh7	Myosin heavy chain 7	Fwd: CAACCTGTCCAAGTTCCGCA
		Rev: GGCATCCTTAGGGTTGGGTAG
Nppa	Natriuretic peptide A	Fwd: CGGCACTTAGCTCCCTCTCT
		Rev: GTTGCAGCCTAGTCCGCTCT
Mef2c	Myocyte-specific enhancer factor 2 C	Fwd: CCAAATCTCCTCCCCCTATGAATC
		Rev: GCTGACGGATATCCTCCCATT
Gata4	GATA binding protein 4	Fwd: CTGTGCCAACTGCCAGACTA
		Rev: AGATTCTTGGGCTTCCGTTT
Srf	Serum response factor	Fwd: CCGTGCTCAATGCCTTCTCT
		Rev: CGTCCAAGTTCACCACCTGTAG
Atp2a2	ATPase Sarcoplasmic/Endoplasmic Reticulum Ca2 + Transporting 2	Fwd: AATCTGGTGACGGATGGTCTG
		Rev: TTCGAAGTCTGGGTTGTCCTC
Cacna1c	Calcium voltage-gated channel subunit alpha1 C	Fwd: AGCAACTTCCCTCAGACGTTTG
		Rev: CACAGTGCTGACCGTGCTG
Pln	Phospholamban	Fwd: TACCTTACTCGCTCGGCTATCAG
		Rev: GACCTTCACGACGATGTCCAG

Table 1. Sequences of primers of target genes used for RT-qPCR.

DTT, 5 mM EDTA, and Halt Protease and Phosphatase Inhibitor Cocktail (Thermo Fisher Scientific). Protein concentrations were determined using DC Protein Assay kits (Bio-Rad) according to the manufacturer's proto-col. Lysates with equal amounts of proteins were run on SDS-PAGE gels and were transferred to polyvinylidene difluoride (Immobilon PVDF; EMD Millipore) or nitrocellulose (Perkin Elmer) membranes. Rabbit anti-ADAP1 antibody (ABS179) was purchased from EMD Millipore. Another antibody directed against a different immu-nogen sequence of ADAP1 (hpa012049) was also tested (data not shown) and was purchased, together with the mouse monoclonal anti-α-actinin antibody (A7811; clone EA-53) from Sigma. Rabbit antibodies directed against GAPDH (5174), ERK1/2 (4695), phospho-ERK1/2 (4370), and MEK1/2 (9122) were purchased from Cell Signaling Technology. Rabbit anti-β1-integrin antibody (sc-8978) was purchased from Santa Cruz Biotechnology. Mouse anti-Hic-5 antibody (611164) was purchased from BD Biosciences. Secondary anti-rabbit-HRP antibody (7074) was purchased from Cell Signaling Technology. Signals were revealed using the Luminata Western HRP Crescendo ECL Substrate purchased from EMD Millipore. Western blot acquisitions and image analyses were performed using a ChemiDoc MP station and Image Lab software (Bio-Rad), respectively.

Protein synthesis assay. Infected RNVC were serum-starved for 48 h and were cultured in methionine-free medium for 1 h prior to performing the assay. The culture medium was then replaced with medium containing 25 µM AHA (Click Chemistry Tools) for 2 h to allow the incorporation of this methionine analog into newly synthesized proteins. Cells were collected in RIPA lysis buffer and equal amount of proteins were labeled with biotin-alkyne according to the manufacturer's protocol (Click Chemistry Tools). Briefly, the following reagents were added to the protein samples at the specified final concentration: 20 µM Biotin-Alkyne (Click Chemistry Tools), 2 mM $CuSO_4$ (Bio Basic), 15 mM ascorbic acid (Fisher Bioreagents), and 5 mM THPTA (Sigma-Aldrich). The samples were incubated for 30 min in the dark and were then boiled in Laemmli buffer for 5 min. Equal amounts of proteins were loaded on SDS-PAGE gels and were analyzed for total biotinylation levels by Western blotting using a streptavidin-HRP conjugate.

Immunofluorescence analysis. RNVC were fixed using 4% paraformaldehyde after 72 h of culture in 96-well imaging microplates (Corning) for cell surface area measurements. RNVC were permeabilized with Triton X-100 and were immunostained with anti-α-actinin primary antibody (cardiomyocyte specific marker, A7811; Sigma) and Alexa Fluor conjugated secondary antibody (4408; Cell Signaling Technology). Images were acquired and analyzed using the Operetta High-Content Imaging System (Perkin Elmer) with a 20X objective. Cell surface areas (in µm²) were measured from technical duplicates (10 fields per well) and were averaged using at least 400 cells per condition. For some experiments, fixed RNVC were also imaged with an Olympus FluoView FV1000 confocal microscope (40X objective; Olympus FV10 ASW 4.0 Viewer analysis software).

Cell surface β1-integrin expression. RNVC were cultured for 72 h post-infection and were washed 3 times with ice-cold PBS (pH 8.0). Cell surface proteins were biotin-labeled at 4 °C for 1 h using the cell-impermeable reagent sulfo-NHS-biotin at a concentration of 0.5 mg/mL in PBS (pH 8.0). The cells were then washed once with ice-cold PBS containing 100 mM glycine for 10 min, followed by 2 washes with ice-cold PBS. The cells were

collected in RIPA lysis buffer, and equal amounts of proteins (600 μg) were incubated with MagReSyn Streptavidin microsphere beads (ReSyn Biosciences) for 2 h at 4 °C. The beads were washed 3 times with wash buffer (80 mM sodium phosphate, 150 mM NaCl, pH 7.5), and were eluted by boiling in biotin-saturated Laemmli buffer for 10 min. Equal volumes of eluted proteins were loaded on an SDS-PAGE gel and were analyzed for cell surface β1-integrin expression by Western blotting as described above.

Statistical analysis. All experiments were performed using at least 3 independent cell isolations. Statistical analyses were performed using GraphPad Prism 7 (GraphPad Software). One-way ANOVA with Tukey's multiple comparison test or two-way ANOVA with Sidak's multiple comparison test were used for hypothesis testing when appropriate. Quantitative data are expressed as means ± standard deviation, and differences with a P value < 0.05 were considered significant.

References

1. Venkateswarlu, K., Brandom, K. G. & Lawrence, J. L. Centaurin-alpha1 is an *in vivo* phosphatidylinositol 3,4,5-trisphosphate-dependent GTPase-activating protein for ARF6 that is involved in actin cytoskeleton organization. *The Journal of biological chemistry* **279**, 6205–6208, https://doi.org/10.1074/jbc.C300482200 (2004).
2. Hammonds-Odie, L. P. *et al*. Identification and cloning of centaurin-alpha. A novel phosphatidylinositol 3,4,5-trisphosphate-binding protein from rat brain. *The Journal of biological chemistry* **271**, 18859–18868 (1996).
3. Dubois, T., Zemlickova, E., Howell, S. & Aitken, A. Centaurin-alpha 1 associates *in vitro* and *in vivo* with nucleolin. *Biochemical and biophysical research communications* **301**, 502–508 (2003).
4. Venkateswarlu, K., Hanada, T. & Chishti, A. H. Centaurin-alpha1 interacts directly with kinesin motor protein KIF13B. *Journal of cell science* **118**, 2471–2484, https://doi.org/10.1242/jcs.02369 (2005).
5. Zemlickova, E. *et al*. Centaurin-alpha(1) associates with and is phosphorylated by isoforms of protein kinase C. *Biochemical and biophysical research communications* **307**, 459–465 (2003).
6. Hayashi, H. *et al*. Centaurin-alpha1 is a phosphatidylinositol 3-kinase-dependent activator of ERK1/2 mitogen-activated protein kinases. *The Journal of biological chemistry* **281**, 1332–1337, https://doi.org/10.1074/jbc.M505905200 (2006).
7. Harada, T. *et al*. AKRL1 and AKRL2 activate the JNK pathway. *Genes to cells: devoted to molecular & cellular mechanisms* **8**, 493–500 (2003).
8. Mutlak, M. & Kehat, I. Extracellular signal-regulated kinases 1/2 as regulators of cardiac hypertrophy. *Frontiers in pharmacology* **6**, 149, https://doi.org/10.3389/fphar.2015.00149 (2015).
9. Hefti, M. A., Harder, B. A., Eppenberger, H. M. & Schaub, M. C. Signaling pathways in cardiac myocyte hypertrophy. *Journal of molecular and cellular cardiology* **29**, 2873–2892, https://doi.org/10.1006/jmcc.1997.0523 (1997).
10. Bueno, O. F. *et al*. The MEK1-ERK1/2 signaling pathway promotes compensated cardiac hypertrophy in transgenic mice. *The EMBO journal* **19**, 6341–6350, https://doi.org/10.1093/emboj/19.23.6341 (2000).
11. Schluter, K. D., Simm, A., Schafer, M., Taimor, G. & Piper, H. M. Early response kinase and PI 3-kinase activation in adult cardiomyocytes and their role in hypertrophy. *The American journal of physiology* **276**, H1655–1663 (1999).
12. Ruwhof, C. & van der Laarse, A. Mechanical stress-induced cardiac hypertrophy: mechanisms and signal transduction pathways. *Cardiovascular research* **47**, 23–37 (2000).
13. Wu, X. *et al*. MEK-ERK pathway modulation ameliorates disease phenotypes in a mouse model of Noonan syndrome associated with the Raf1(L613V) mutation. *The Journal of clinical investigation* **121**, 1009–1025, https://doi.org/10.1172/JCI44929 (2011).
14. Cai, J. *et al*. Crocetin protects against cardiac hypertrophy by blocking MEK-ERK1/2 signalling pathway. *Journal of cellular and molecular medicine* **13**, 909–925, https://doi.org/10.1111/j.1582-4934.2008.00620.x (2009).
15. Lawrence, J., Mundell, S. J., Yun, H., Kelly, E. & Venkateswarlu, K. Centaurin-alpha 1, an ADP-ribosylation factor 6 GTPase activating protein, inhibits beta 2-adrenoceptor internalization. *Molecular pharmacology* **67**, 1822–1828, https://doi.org/10.1124/mol.105.011338 (2005).
16. Moore, C. D. *et al*. The neuronal Arf GAP centaurin alpha1 modulates dendritic differentiation. *Journal of cell science* **120**, 2683–2693, https://doi.org/10.1242/jcs.006346 (2007).
17. D'Souza-Schorey, C., Li, G., Colombo, M. I. & Stahl, P. D. A regulatory role for ARF6 in receptor-mediated endocytosis. *Science* **267**, 1175–1178 (1995).
18. Honda, A. *et al*. Phosphatidylinositol 4-phosphate 5-kinase alpha is a downstream effector of the small G protein ARF6 in membrane ruffle formation. *Cell* **99**, 521–532 (1999).
19. D'Souza-Schorey, C. & Chavrier, P. ARF proteins: roles in membrane traffic and beyond. *Nature reviews. Molecular cell biology* **7**, 347–358, https://doi.org/10.1038/nrm1910 (2006).
20. Powelka, A. M. *et al*. Stimulation-dependent recycling of integrin beta1 regulated by ARF6 and Rab11. *Traffic* **5**, 20–36 (2004).
21. Hongu, T. *et al*. Arf6 regulates tumour angiogenesis and growth through HGF-induced endothelial beta1 integrin recycling. *Nature communications* **6**, 7925, https://doi.org/10.1038/ncomms8925 (2015).
22. Pham, C. G. *et al*. Striated muscle-specific beta(1D)-integrin and FAK are involved in cardiac myocyte hypertrophic response pathway. *American journal of physiology. Heart and circulatory physiology* **279**, H2916–2926 (2000).
23. Brancaccio, M. *et al*. Integrin signalling: the tug-of-war in heart hypertrophy. *Cardiovascular research* **70**, 422–433, https://doi.org/10.1016/j.cardiores.2005.12.015 (2006).
24. Ross, R. S. *et al*. Beta1 integrins participate in the hypertrophic response of rat ventricular myocytes. *Circ Res* **82**, 1160–1172 (1998).
25. Krishnamurthy, P., Subramanian, V., Singh, M. & Singh, K. Beta1 integrins modulate beta-adrenergic receptor-stimulated cardiac myocyte apoptosis and myocardial remodeling. *Hypertension* **49**, 865–872, https://doi.org/10.1161/01.HYP.0000258703.36986.13 (2007).
26. Pinto, A. R. *et al*. Revisiting Cardiac Cellular Composition. *Circ Res* **118**, 400–409, https://doi.org/10.1161/CIRCRESAHA.115.307778 (2016).
27. Simpson, P., McGrath, A. & Savion, S. Myocyte hypertrophy in neonatal rat heart cultures and its regulation by serum and by catecholamines. *Circ Res* **51**, 787–801 (1982).
28. Chien, K. R., Knowlton, K. U., Zhu, H. & Chien, S. Regulation of cardiac gene expression during myocardial growth and hypertrophy: molecular studies of an adaptive physiologic response. *FASEB journal: official publication of the Federation of American Societies for Experimental Biology* **5**, 3037–3046 (1991).
29. Kuwahara, K., Nishikimi, T. & Nakao, K. Transcriptional regulation of the fetal cardiac gene program. *Journal of pharmacological sciences* **119**, 198–203 (2012).
30. Gillespie-Brown, J., Fuller, S. J., Bogoyevitch, M. A., Cowley, S. & Sugden, P. H. The mitogen-activated protein kinase kinase MEK1 stimulates a pattern of gene expression typical of the hypertrophic phenotype in rat ventricular cardiomyocytes. *The Journal of biological chemistry* **270**, 28092–28096 (1995).
31. Kodama, H. *et al*. Significance of ERK cascade compared with JAK/STAT and PI3-K pathway in gp130-mediated cardiac hypertrophy. *American journal of physiology. Heart and circulatory physiology* **279**, H1635–1644 (2000).

32. Liang, F., Lu, S. & Gardner, D. G. Endothelin-dependent and -independent components of strain-activated brain natriuretic peptide gene transcription require extracellular signal regulated kinase and p38 mitogen-activated protein kinase. *Hypertension* **35**, 188-192 (2000).

33. Munzel, F. *et al*. Endothelin-1 and isoprenaline co-stimulation causes contractile failure which is partially reversed by MEK inhibition. *Cardiovascular research* **68**, 464–474, https://doi.org/10.1016/j.cardiores.2005.06.020 (2005).

34. Kim, D. J. *et al*. Cellular localization of integrin isoforms in phenylephrine-induced hypertrophic cardiac myocytes. *Cell biochemistry and function* **21**, 41–48, https://doi.org/10.1002/cbf.988 (2003).

35. Yund, E. E., Hill, J. A. & Keller, R. S. Hic-5 is required for fetal gene expression and cytoskeletal organization of neonatal cardiac myocytes. *Journal of molecular and cellular cardiology* **47**, 520–527, https://doi.org/10.1016/j.yjmcc.2009.06.006 (2009).

36. Aggensteiner, M. & Reiser, G. Expression of the brain-specific membrane adapter protein p42IP4/centaurin alpha, a Ins(1,3,4,5)P4/PtdIns(3,4,5)P3 binding protein, in developing rat brain. *Brain research. Developmental brain research* **142**, 77–87 (2003).

37. Whitley, P. *et al*. Identification of centaurin-alpha2: a phosphatidylinositide-binding protein present in fat, heart and skeletal muscle. *European journal of cell biology* **81**, 222–230 (2002).

38. Uhlen, M. *et al*. Proteomics. Tissue-based map of the human proteome. *Science* **347**, 1260419, https://doi.org/10.1126/science.1260419 (2015).

39. Cohen, L. D. *et al*. Metabolic turnover of synaptic proteins: kinetics, interdependencies and implications for synaptic maintenance. *PloS one* **8**, e63191, https://doi.org/10.1371/journal.pone.0063191 (2013).

40. Venkateswarlu, K., Oatey, P. B., Tavare, J. M., Jackson, T. R. & Cullen, P. J. Identification of centaurin-alpha1 as a potential *in vivo* phosphatidylinositol 3,4,5-trisphosphate-binding protein that is functionally homologous to the yeast ADP-ribosylation factor (ARF) GTPase-activating protein, Gcs1. *The Biochemical journal* **340**(Pt 2), 359–363 (1999).

41. Szatmari, E. M., Oliveira, A. F., Sumner, E. J. & Yasuda, R. Centaurin-alpha1-Ras-Elk-1 signaling at mitochondria mediates beta-amyloid-induced synaptic dysfunction. *The Journal of neuroscience: the official journal of the Society for Neuroscience* **33**, 5367–5374, https://doi.org/10.1523/JNEUROSCI.2641-12.2013 (2013).

42. Kehat, I. *et al*. Extracellular signal-regulated kinases 1 and 2 regulate the balance between eccentric and concentric cardiac growth. *Circ Res* **108**, 176–183, https://doi.org/10.1161/CIRCRESAHA.110.231514 (2011).

43. Fujio, Y., Nguyen, T., Wencker, D., Kitsis, R. N. & Walsh, K. Akt promotes survival of cardiomyocytes *in vitro* and protects against ischemia-reperfusion injury in mouse heart. *Circulation* **101**, 660–667 (2000).

44. Padmasekar, M., Nandigama, R., Wartenberg, M., Schluter, K. D. & Sauer, H. The acute phase protein alpha2-macroglobulin induces rat ventricular cardiomyocyte hypertrophy via ERK1,2 and PI3-kinase/Akt pathways. *Cardiovascular research* **75**, 118–128, https://doi.org/10.1016/j.cardiores.2007.03.003 (2007).

45. Robert, P. *et al*. EDG1 receptor stimulation leads to cardiac hypertrophy in rat neonatal myocytes. *Journal of molecular and cellular cardiology* **33**, 1589–1606, https://doi.org/10.1006/jmcc.2001.1433 (2001).

46. Morimoto, T. *et al*. Phosphorylation of GATA-4 is involved in alpha 1-adrenergic agonist-responsive transcription of the endothelin-1 gene in cardiac myocytes. *The Journal of biological chemistry* **275**, 13721–13726 (2000).

47. Tenhunen, O. *et al*. Mitogen-activated protein kinases p38 and ERK 1/2 mediate the wall stress-induced activation of GATA-4 binding in adult heart. *The Journal of biological chemistry* **279**, 24852–24860, https://doi.org/10.1074/jbc.M314317200 (2004).

48. Ueyama, T. *et al*. Requirement of activation of the extracellular signal-regulated kinase cascade in myocardial cell hypertrophy. *Journal of molecular and cellular cardiology* **32**, 947–960, https://doi.org/10.1006/jmcc.2000.1135 (2000).

49. Thacker, E. *et al*. Thearf6 GAP centaurin alpha-1 is a neuronal actin-binding protein which also functions via GAP-independent activity to regulate the actin cytoskeleton. *European journal of cell biology* **83**, 541–554 (2004).

50. Sarantitis, I., Papanastasopoulos, P., Manousi, M., Baikoussis, N. G. & Apostolakis, E. The cytoskeleton of the cardiac muscle cell. *Hellenic journal of cardiology: HJC=Hellenike kardiologike epitheorese* **53**, 367–379 (2012).

51. Israeli-Rosenberg, S., Manso, A. M., Okada, H. & Ross, R. S. Integrins and integrin-associated proteins in the cardiac myocyte. *Circ Res* **114**, 572–586, https://doi.org/10.1161/CIRCRESAHA.114.301275 (2014).

52. Vitali, T., Girald-Berlingeri, S., Randazzo, P. A. & Chen, P. W. Arf GAPs: A family of proteins with disparate functions that converge on a common structure, the integrin adhesion complex. *Small GTPases*, 1–9, https://doi.org/10.1080/21541248.2017.1299271 (2017).

53. Sato, H., Suzuki-Inoue, K., Inoue, O. & Ozaki, Y. Regulation of adaptor protein GIT1 in platelets, leading to the interaction between GIT1 and integrin alpha(IIb)beta3. *Biochemical and biophysical research communications* **368**, 157–161, https://doi.org/10.1016/j.bbrc.2008.01.064 (2008).

54. Chan, S. H. *et al*. MicroRNA-149 targets GIT1 to suppress integrin signaling and breast cancer metastasis. *Oncogene* **33**, 4496–4507, https://doi.org/10.1038/onc.2014.10 (2014).

55. Li, J., *et al*. Phosphorylation of ACAP1 by Akt regulates the stimulation-dependent recycling of integrin beta1 to control cell migration. *Developmental cell* **9**, 663–673, https://doi.org/10.1016/j.devcel.2005.09.012 (2005).

56. Kondo, A. *et al*. A new paxillin-binding protein, PAG3/Papalpha/KIAA0400, bearing an ADP-ribosylation factor GTPase-activating protein activity, is involved in paxillin recruitment to focal adhesions and cell migration. *Molecular biology of the cell* **11**, 1315–1327 (2000).

57. Eble, D. M. *et al*. Endothelin-induced cardiac myocyte hypertrophy: role for focal adhesion kinase. *American journal of physiology. Heart and circulatory physiology* **278**, H1695–1707 (2000).

58. Sbroggio, M. *et al*. ERK1/2 activation in heart is controlled by melusin, focal adhesion kinase and the scaffold protein IQGAP1. *Journal of cell science* **124**, 3515–3524, https://doi.org/10.1242/jcs.091140 (2011).

59. Livak, K. J. & Schmittgen, T. D. Analysis of relative gene expression data using real-time quantitative PCR and the 2(-Delta Delta C(T)) Method. *Methods* **25**, 402–408, https://doi.org/10.1006/meth.2001.1262 (2001).

Acknowledgements

Author Contributions

H.G. and M.A.-M. designed the experiments; H.G., A.-A.D., J.B., V.O. and G.L. conducted the experiments; H.G. and A.-A.D. analyzed the results; and H.G. and M.A.-M. supervised the research and wrote the paper. All authors reviewed the manuscript.

Additional Information

Supplementary information accompanies this paper at https://doi.org/10.1038/s41598-018-31784-w.

Competing Interests: The authors declare no competing interests.

Publisher's note: Springer Nature remains neutral with regard to jurisdictional claims in published maps and institutional affiliations.